nature climate change

Article

https://doi.org/10.1038/s41558-023-01893-0

Climate warming restructures food webs and carbon flow in high-latitude ecosystems

Received: 19 May 2023

Accepted: 15 November 2023

Published online: 3 January 2024

Check for updates

Philip J. Manlick[1,2,3] ✉, Nolan L. Perryman[2,4], Amanda M. Koltz[5], Joseph A. Cook[2,3] & Seth D. Newsome[2]

Rapid warming of high-latitude ecosystems is increasing microbial activity and accelerating the decomposition of permafrost soils. This proliferation of microbial energy could restructure high-latitude food webs and alter carbon cycling between above-ground and below-ground habitats. We used stable isotope analysis ($\delta^{13}C$) of amino acids to trace carbon flow through food webs exposed to warming and quantified changes in the assimilation of microbial carbon by Arctic tundra and boreal forest consumers. From 1990 to 2021, small mammals in boreal forests exhibited a significant reduction in the use of plant-based 'green' food webs and an increased use of microbially mediated 'brown' food webs, punctuated by a >30% rise in fungal carbon assimilation. Similarly, fungal carbon assimilation rose 27% in wolf spiders under experimental warming in Arctic tundra. These findings reveal a climate-mediated 'browning' of high-latitude food webs and point to an understudied pathway by which animals can impact carbon cycling under climate warming.

High-latitude ecosystems are warming at unparalleled rates, with widespread consequences for ecological processes[1–3]. Of particular concern is thawing permafrost and the release of long-sequestered carbon (C) from northern soils that can lead to C-cycle feedbacks, thereby accelerating rising temperatures[4,5]. Permafrost covers ~25% of Earth's terrestrial surface and stores nearly twice as much C as is currently in the atmosphere[5], but climatic warming has increased microbial decomposition of this previously frozen soil organic matter, resulting in increased heterotrophic respiration and greenhouse gas emissions[6,7]. While the consequences of this 'microbial awakening' for C cycling have received widespread attention[4,5,8], the impact of climate-mediated permafrost decay on high-latitude terrestrial food webs remains unclear[9].

Permafrost decomposition and subsequent increases in microbial activity could restructure high-latitude food webs by altering the availability of C sources and energy channels accessible to consumers[9]. For example, ancient C leached from permafrost soils as dissolved organic carbon can subsidize aquatic food webs via assimilation by heterotrophic microbes, thereby altering resource pathways and energy channelling across ecosystems[10,11]. At the same time, increases in primary production due to climate warming have precipitated widespread 'greening' across high-latitude ecosystems, potentially increasing the availability of plant-based energy channels[12,13]. However, the extents to which greening and microbial decomposition of permafrost impact energy flow and consumers in terrestrial food webs remains largely unknown[14]. Although terrestrial food webs have historically been categorized as either above-ground 'green' webs supported by plants or below-ground 'brown' webs fuelled by detritus, accumulating evidence suggests green and brown food webs are interlinked and that microbially mediated energy supports higher-order consumers in both above- and below-ground systems[15–17]. For example, small mammals in a montane ecosystem acquire nearly 70% of their energy from microbial sources[17], while energetic models suggest invertebrate food webs in Arctic tundra are supported almost entirely by fungal energy channels[18]. In their seminal assessment of a high-Arctic ecosystem, Summerhayes and Elton[19] also recognized that animals connect above- and below-ground food webs, a linkage that has been corroborated by contemporary studies[20]. Thus, it stands to reason that climate-mediated permafrost decay and the rapid proliferation of microbial energy

[1]Pacific Northwest Research Station, USDA Forest Service, Juneau, AK, USA. [2]Department of Biology, University of New Mexico, Albuquerque, NM, USA. [3]Museum of Southwestern Biology, University of New Mexico, Albuquerque, NM, USA. [4]SWCA Environmental Consultants, Albuquerque, NM, USA. [5]Department of Integrative Biology, University of Texas at Austin, Austin, TX, USA. ✉e-mail: philip.manlick@usda.gov

https://doi.org/10.1038/s41558-023-01893-0

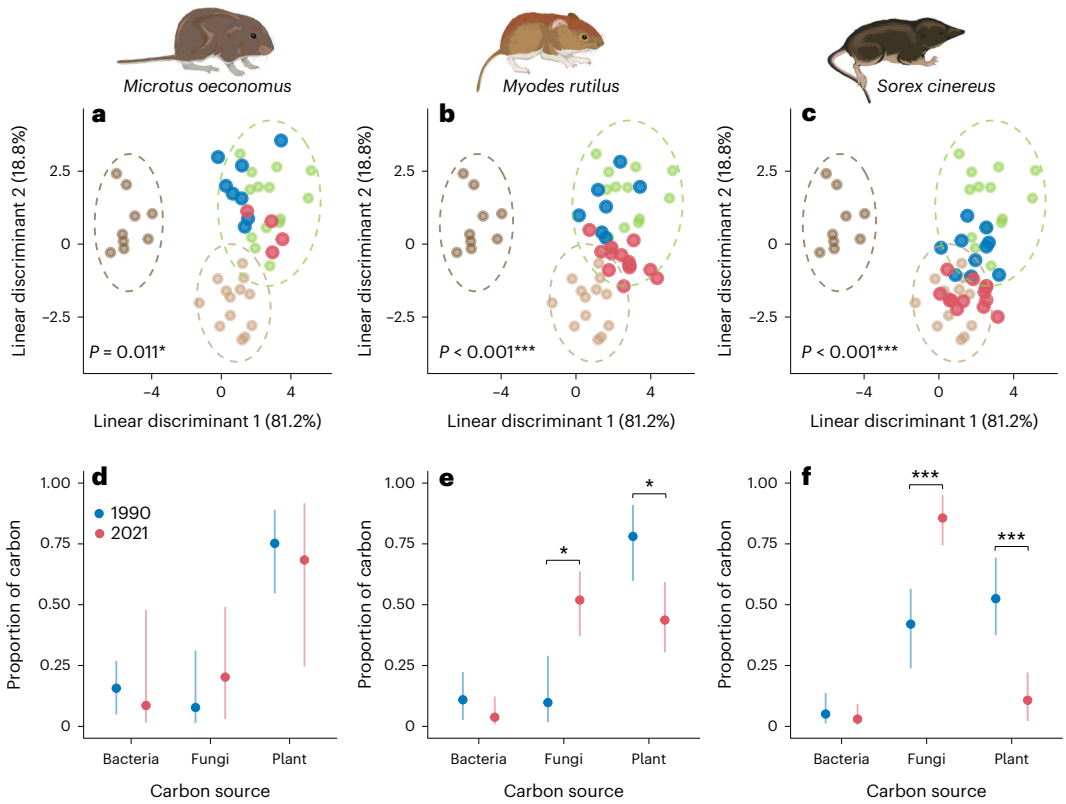

Fig. 1 | Food-web structure and carbon flow in boreal forest mammals. **a**–**c**, Linear discriminant analysis (LDA) of carbon sources and small mammals from Alaskan boreal forest. Carbon sources included plants (green; $N = 14$), fungi (light brown; $N = 13$) and bacteria (dark brown; $N = 10$), and mammals included tundra (*Microtus oeconomus*; $N_{1990} = 8$ and $N_{2021} = 4$) (**a**,**d**), red-backed voles (*Myodes rutilus*; $N_{1990} = 7$ and $N_{2021} = 13$) (**b**,**e**) and masked shrews (*Sorex cinereus*; $N_{1990} = 10$ and $N_{2021} = 13$) (**c**,**f**) collected in 1990 (blue) and 2021 (red). Standard ellipse areas (95%) for carbon sources are represented by dashed lines, percentage of variation described by linear discriminants is reported in parentheses and *P* values represent multivariate differences in linear discriminant means between 1990 and 2021 assessed via PERMANOVA. **d**–**f**, Mean proportion of carbon assimilated by mammals represented by solid dots, with 95% credible intervals represented by solid lines. Significant differences between periods were determined via two-sided *t* tests corrected for multiple comparisons and are noted by asterisks. LDA and proportional estimates per species are aligned vertically. Illustrations by Juliana Masseloux.

channels in below-ground ecosystems may subsidize above-ground consumers and restructure high-latitude food webs, with potential consequences for ecosystem processes such as nutrient cycling[9].

The coupling of green and brown food webs by animal consumers represents a direct channel between above- and below-ground C pools that can alter nutrient cycling[16,21]. Animals play important but often underappreciated roles in C cycling through numerous direct and indirect processes, including herbivory, predation and waste production[22–25]. For example, large ungulates and microtine rodents can directly limit C storage through herbivory that reduces primary production[24,26,27], while the consumptive[28] and non-consumptive[29] effects of predators often govern energy flow and C storage in above- and below-ground compartments. The flow of C between above- and below-ground systems via the coupling of green and brown food webs has similar potential to impact C cycling through the transfer and storage of C in different trophic compartments, but quantification of these fluxes remains limited[23,25].

In this Article, we employ an emerging technique—essential amino acid (EAA) carbon isotope ($\delta^{13}C$) fingerprinting[30]—to quantify the impact of climate warming on energy flow and C fluxes between green and brown food webs in Arctic tundra and boreal forests in Alaska, USA. We use $\delta^{13}C$ analysis of EAAs to trace the flow of C through food webs, quantify the proportional assimilation of green and brown C by above-ground consumers and estimate C fluxes between trophic compartments on the basis of food-web shifts[30–32]. EAAs are ideal biomarkers to trace the flow of C through terrestrial food webs because they can be synthesized only by bacteria, fungi and plants, each via unique enzymatic pathways that impart distinct patterns, or 'fingerprints', among $\delta^{13}C$ values[31]. Animals cannot synthesize EAAs de novo and therefore must assimilate these biomolecules from their diet. Because EAAs are limiting, EAA $\delta^{13}C$ fingerprints are transferred through food webs and assimilated by consumers with minimal isotopic alteration, thereby enabling the quantification of carbon flow through food webs[30,32]. Further, the majority of vertebrate biomass is bound in amino acids as protein[33], and EAA $\delta^{13}C$ fingerprints provide a reliable proxy for the assimilation of green versus brown energy by consumers across species and systems[17,30].

We use EAA $\delta^{13}C$ fingerprinting to quantify proportional changes in C flow and connectivity between green and brown food webs using two high-latitude consumer guilds subjected to long-term and short-term climate warming: (1) small-mammal specimens from a boreal forest separated by 30 years of rising temperatures[34] and (2) wolf spiders (*Pardosa* spp.) from experimentally warmed mesocosms in the Arctic tundra. Small-mammal bone collagen was sampled from museum specimens collected in 1990 and 2021 near Fairbanks, Alaska, where temperatures rose 1.4 °C in the twentieth century[34]. Specimens included two rodents, herbivorous tundra voles (*Microtus oeconomus*) and omnivorous (often fungivorous) northern red-backed voles (*Myodes rutilus*), as well as masked shrews (*Sorex cinereus*), an insectivorous predator of the soil food web[35,36]. Wolf spiders are generalist predators of invertebrate prey from the soil food web[37] and were sampled near Toolik Lake, Alaska, in 2013 from paired control and passively warmed mesocosm plots whose summertime temperatures differed by approximately 2 °C[38]. We tested for differences in C assimilation between periods and treatments,

and we predicted that the proportion of brown C (bacteria and fungi) assimilated by consumers would be higher under warming conditions due to the greater availability of microbial energy from increased decomposition of permafrost soils. We then used radiocarbon dating of small-mammal bone collagen to estimate the age and source of assimilated C, and we used measured differences in the proportions of green and brown C assimilated by consumers under warming to estimate C fluxes due to climate-mediated food-web shifts.

Food webs and carbon flow

We detected widespread changes in C assimilation by small mammals exposed to long-term warming in a boreal forest, highlighted by a significant shift from plant- to fungal-based food webs (Fig. 1a–c). Multivariate differences in linear discriminant means between 1990 and 2021 revealed significant shifts in masked shrews ($F_{1,22} = 11.1$, $P > 0.001$), red-backed voles ($F_{1,19} = 13.1$, $P > 0.001$) and tundra voles ($F_{1,11} = 6.6$, $P = 0.011$). Further, shrews, red-backed voles and tundra voles also exhibited 43.8%, 40.3% and 11.6% increases in fungal C assimilation, respectively (Supplementary Table 1). For example, the mean proportion of fungal C assimilated by omnivorous red-backed voles in 1990 was 0.11 ± 0.07 (s.d.), with plants providing the primary C source (0.77 ± 0.08). By 2021, fungal energy had increased significantly and was the primary C source for red-backed voles (0.51 ± 0.07; $P = 0.01$), directly offset by a >30% reduction in assimilated plant C (0.44 ± 0.07; $P = 0.02$; Fig. 1e). Predatory shrews also exhibited significant increases in the assimilation of fungal C through time (Fig. 1f), such that fungal C dominated contemporary samples (0.85 ± 0.05; $P = 0.02$) and was offset by a >40% decline in plant C contributions from 1990 to 2021 ($P < 0.001$). Despite modest increases in fungal C assimilation, herbivorous tundra voles did not exhibit significant shifts in C sources ($P = 0.60$; Fig. 1d), assimilating primarily plant C in both 1990 (0.74 ± 0.09) and 2021 (0.66 ± 0.17). Notably, bacterial C contributions represented <20% of the assimilated C for all small mammals across periods, and all species exhibited a small but non-significant decrease ($\bar{x} = 4.1\%$; all $P > 0.40$) in bacterial C assimilation from 1990 to 2021 (Supplementary Table 1).

Arctic wolf spiders displayed an almost identical shift from plant- to fungal-based food webs under experimental warming (Fig. 2a; $F_{1,31} = 5.6$, $P = 0.009$), with a 27.4% increase in assimilated fungal C between control (0.26 ± 0.08) and treatment (0.53 ± 0.07) animals (Fig. 2b; $P = 0.02$). This increase in fungal C assimilation was directly offset by a 26.1% decrease in assimilated plant C, declining from 0.68 ± 0.07 to 0.42 ± 0.06 in control and treatment spiders, respectively (Fig. 2b; $P = 0.02$). Assimilation of bacterial C by spiders did not change ($P = 0.79$), and proportional use remained low (≤0.06) for both control and warming treatments (Fig. 2b and Supplementary Table 1).

To estimate the assimilation of ancient C from permafrost, we compared radiocarbon ($\Delta^{14}C$) for a subset of each small-mammal species ($N = 18$) from 1990 and 2021 to atmospheric levels during the same time periods (Fig. 3). We detected significant enrichment in mean (± SD) $\Delta^{14}C$ of consumers from 1990 ($\Delta^{14}C_{consumer} = 172.5‰ \pm 19.7$; $\Delta^{14}C_{atmosphere} = 149.2‰ \pm 4.5$; $p = 0.007$) and 2021 ($\Delta^{14}C_{consumer} = 12.0‰ \pm 6.5$; $\Delta^{14}C_{atmosphere} = 0.6‰ \pm 1.2$; $p = 0.001$) compared to mean atmospheric levels at the same times, indicating that all animals were composed primarily of modern C.

Carbon fluxes between food webs

The quantification of carbon flow and assimilation by consumers has considerable potential to inform food-web and C-cycle models that require estimates of biomass and C flow between trophic compartments[23,25]. To demonstrate the utility of our approach for these models, we estimated brown C pools and fluxes driven by red-backed vole populations between 1990 and 2021. Northern red-backed voles are a broadly distributed Holarctic rodent typified by generalist, often mycophagous, foraging behaviour and eruptive population dynamics[36,39]. Consequently, changes in energy channelling by red-backed voles have

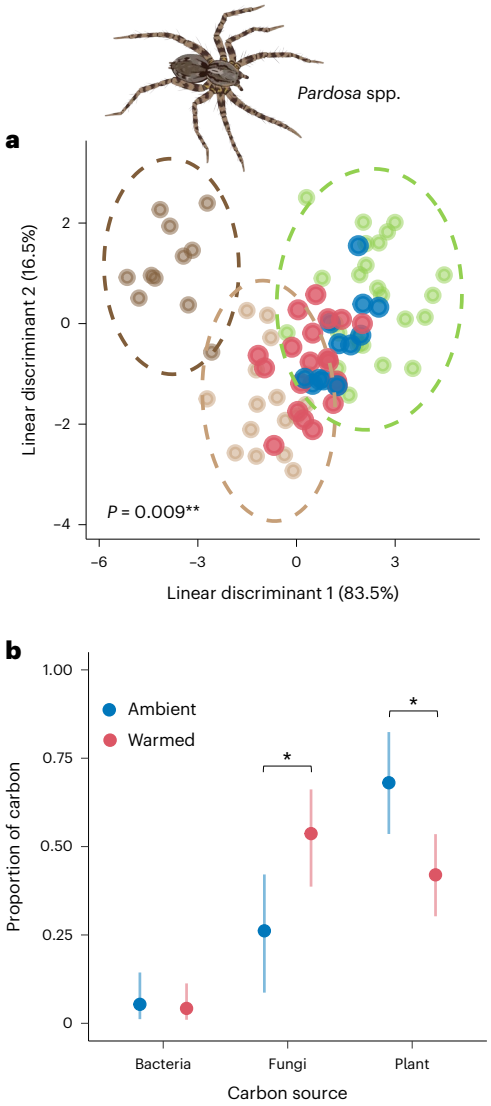

Fig. 2 | Food-web structure and carbon flow in Arctic wolf spiders. a, LDA of carbon sources and wolf spiders (*Pardosa* spp.) from the Alaskan Arctic tundra. Carbon sources included plants (green; $N = 24$), fungi (light brown; $N = 16$) and bacteria (dark brown; $N = 12$), and wolf spiders were collected from ambient ($N = 12$, blue) and warmed ($N = 20$, red) mesocosms. Standard ellipse areas (95%) for carbon sources are represented by dashed lines, percentage variation described by each linear discriminant is reported in parentheses and *P* values represent multivariate differences in linear discriminant means between ambient and warmed plots assessed via PERMANOVA. **b**, Mean proportion of carbon assimilated by wolf spiders represented by solid dots, with 95% credible intervals represented by solid lines. Significant differences between treatments were determined via two-sided *t* tests corrected for multiple comparisons and are noted by asterisks. Illustration by Juliana Masseloux.

the potential to alter linkages between green and brown food webs and drive above-ground–below-ground C fluxes. We estimate that the pool of stored C in contemporary red-backed vole populations from boreal Alaska contains 40% more brown C than in the late twentieth century. Given an average mass of 21.6 ± 5.5 g and a measured C concentration of 50.6% in vole tissues, the average population of red-backed voles[39] stored twice as much brown C in 2021 (9.2 ± 5.9 mgC m^{-2}) as it did in 1990 (3.7 ± 2.9 mgC m^{-2}), and we estimate the transfer of C from below-ground brown food webs to above-ground vole populations was approximately 5,505.3 gC km^{-2} from 1990 to 2021.

Wolf spiders are prominent predators of the Arctic tundra and acquire much of their energy from brown food webs[18,37]. Koltz et al.[37]

https://doi.org/10.1038/s41558-023-01893-0

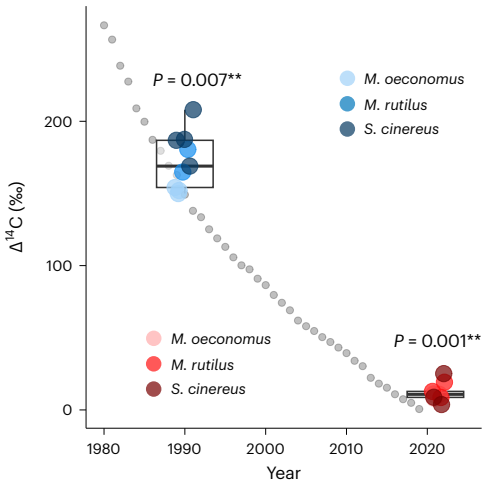

Fig. 3 | Carbon assimilated by boreal forest mammals. Radiocarbon values ($\Delta^{14}C$) for small-mammal specimens from 1990 ($N = 9$, blue) and 2021 ($N = 9$, red) plotted relative to mean atmospheric $\Delta^{14}C$ (gray) from 1980 to 2019. Black lines represent median values for mammals in each period, boxes represent the interquartile range and whiskers represent minimum and maximum values. Shades represent different species within each period, and *P* values reflect differences between small mammals and atmospheric $\Delta^{14}C$ for each period as determined via two-sided *t* test.

estimated a standing spider biomass of 4,360 g km^{-2} in moist acidic tundra habitat across the North Slope of Alaska. Given an average wolf spider C concentration of 51.8% ± 5.3, we estimate that wolf spiders stored nearly twice as much brown C in warmed plots (1.31 ± 0.22 mgC m^{-2}) versus control plots (0.72 ± 0.22 mgC m^{-2}). If tundra ecosystems increase by a uniform 2 °C comparable to experimental mesocosm conditions, these results suggest >30% of the standing pool of wolf spider biomass in this region could be composed of brown C.

Discussion

We present clear evidence that climate warming alters C flow and food-web dynamics among above-ground consumers in Arctic tundra and boreal forest ecosystems, and we show that these changes are the consequence of a state change from predominantly green, plant-based food webs to brown, microbe-based food webs. These results demonstrate that animals play key functional roles in nutrient cycling by linking trophic compartments across green and brown food webs, and that climate-mediated changes in food-web coupling can redistribute C between above- and below-ground pools. The observed food-web shifts and functional responses were consistent across species, ecosystems, and long- and short-term warming scenarios. Collectively, these findings suggest climate change is reshaping high-latitude terrestrial food webs, with direct implications for ecosystem processes.

Food-web shifts in our Arctic tundra and boreal forest ecosystems were driven almost entirely by an increased use of fungal energy channels by above-ground consumers. This reliance on fungal energy is consistent with studies showing that fungi regulate the coupling of green and brown food webs in boreal forest and Arctic tundra ecosystems[17,18,40,41]. Using an energetic food-web model, Koltz et al.[18] estimated that >90% of C in contemporary invertebrate tundra food webs is routed through fungal channels and predicted that above-ground predators such as wolf spiders acquire up to 46% of their energy from brown sources. Our results suggest this number may be substantially higher and is mediated by climate, with predatory spiders and shrews assimilating 53% and 85% brown C under warming conditions, respectively. As generalist apex predators at the interface of above-ground and below-ground ecosystems[17,42], shrews and spiders are reliable integrators of trophic interactions and reflect changes in energy flow through the food web. Our results therefore indicate that climate-mediated increases in fungal C assimilation are an ecosystem-level phenomenon that extends beyond the consumer species measured herein.

We postulate that the observed transfer of brown C to above-ground consumers is the result of multiple trophic interactions following decomposition of organic matter by fungi at the base of the food web[17]. Fungi are primary decomposers of plant biomass and soil organic matter in both boreal forests[43] and recently thawed permafrost[40,44], where they transform recalcitrant biomass (for example, cellulose and lignin) into labile biomolecules such as amino acids that are more readily assimilated by both plants and animals[17,45]. This fungal energy channel represents a substantial portion of the assimilable energy in terrestrial ecosystems[46]. In turn, fungal-feeding detritivores such as collembola, oligochaetes and oribatid mites directly consume and assimilate fungal C before transferring this energy to higher trophic level consumers such as wolf spiders and shrews via predation[18,37,42]. While we did not directly characterize consumer diet composition, we suggest that intermediary invertebrate consumers regulate the flow of brown C to apex predators, thereby mediating the type and proportion of C assimilated by predatory consumers[17,37]. In addition, fungivorous consumers such as red-backed voles may directly consume and assimilate fungal sporocarps[39], and the availability of this resource could increase with warming and elevated rainfall in high-latitude systems[47,48]. Given that the proportion of fungal to bacterial decomposition tends to increase with warming[44,49,50], we expect the observed shifts in energy flow through fungal channels to persist under predicted future climates[47]. To this point, we analysed small-mammal bone collagen, which integrates isotopic signatures over the majority of an animal's life[30], confirming that the observed increases in fungal C were the result of prolonged assimilation and not seasonal exploitation.

The importance of animals in C cycling has received considerable debate, but it is increasingly recognized that animals impact C fluxes and pools through direct and indirect processes[22–25]. We used an emerging stable isotope approach to empirically trace C through food webs, and our results point to an underexplored pathway by which animals may alter C cycling—climate-mediated shifts in animal foraging that redistribute C between above- and below-ground pools. For example, we show that a single omnivorous species, red-backed voles, can redirect brown C from below-ground to above-ground trophic compartments and that this flux of brown C has increased with climate warming. This redistribution of brown C was consistent across all consumers, suggesting the total flux of brown C to above-ground trophic compartments is probably orders of magnitude higher than estimates herein after accounting for the broader consumer community. Beyond the direct transport of C, shifts in trophic interactions and energy channelling by consumers can have indirect effects on nutrient cycling and ecosystem function that probably outweigh direct effects. For example, using the same mesocosm experiment outlined in the preceding, Koltz et al.[37] showed that warming altered a trophic cascade among wolf spiders and their collembola prey, ultimately leading to less decomposition. Our data corroborate these findings and suggest above-ground predators exert top-down influence on below-ground prey that can impact nutrient cycling and C storage via both direct and indirect mechanisms that warrant additional attention. Climate warming also decreased the use of plant C among all consumers, which may reflect reduced herbivory and top-down pressure on primary producers. For example, voles can significantly reduce net primary production[24,26], indicating that the observed declines in assimilated plant C by tundra voles (8.3%) and red-backed voles (33.4%) could also increase C storage in above-ground compartments through changes in herbivory. Theoretical models similarly predict that climate change will rewire trophic interactions and alter the distribution of C across trophic compartments[23,51,52], but these changes are rarely quantified in empirical studies. We outline a novel approach to quantify the magnitude and directionality of C flow between trophic compartments, a framework

that could ultimately be used to parameterize food-web modules and 'animate' the carbon cycle[23].

Our radiocarbon data revealed that there has not been a shift in the type of C utilized by terrestrial consumers in boreal ecosystems from 1990 to 2021. Previous work has shown that as permafrost decays, it releases ancient C that can subsidize contemporary aquatic food webs[11]. We expected that terrestrial consumers would exhibit a similar pattern, but instead found that both historical and contemporary animals assimilated modern C. While overall trends in assimilated ^{14}C by consumers did not indicate contributions of ancient permafrost C, significant enrichment of consumers relative to atmospheric levels suggests animals assimilate slightly older C that was fixed in preceding years[53]. Although contrary to initial predictions, this result is consistent with ^{14}C measurements in boreal forests where respired and below-ground CO_2 from decomposing permafrost is composed almost exclusively of modern C, while undisturbed permafrost may contain C dated to >1,000 yr BP (ref. 54). Moreover, previous research in our study area has shown that ancient C is respired faster than modern C[7] and that ancient C is often mobilized as dissolved organic carbon before being integrated into aquatic systems[11,54]. It is also possible that warming-induced increases in primary production across high-latitude ecosystems (Arctic greening) has led to greater leaf litter inputs[12,55], thereby stimulating fungal decomposition of contemporary plant matter and the routing of modern C to small-mammal consumers. Understanding the relative impacts of permafrost decay and increased primary production on C flow will be critical to identifying the mechanisms regulating changes in food-web coupling and nutrient cycling.

This study adds to a growing body of literature illustrating that animals link green and brown food webs[17,18] and shows that climate warming consistently alters the coupling of these energy channels across species and ecosystems. Establishing the trophic pathways by which changes in energy channelling occur remains elusive, however, as are direct links to ecosystem processes such as nutrient cycling. In this Article, we demonstrate that sources of energy and the flow of carbon between above-ground and below-ground ecosystems can be identified through isotopic analysis of essential amino acids, and we outline a promising approach for expanding our understanding of global change impacts on food webs and their energetics. Lastly, while a multitude of studies have identified broad-scale patterns of greening in northern ecosystems[12,13], our study reveals a concurrent browning of above-ground food webs. Disentangling the processes linking these emergent phenomena is needed to develop a mechanistic understanding of ongoing ecological change in high-latitude ecosystems.

Online content

Any methods, additional references, Nature Portfolio reporting summaries, source data, extended data, supplementary information, acknowledgements, peer review information; details of author contributions and competing interests; and statements of data and code availability are available at https://doi.org/10.1038/s41558-023-01893-0.

References

1. IPCC *Climate Change 2013: The Physical Science Basis* (eds Stocker, T. F. et al.) (Cambridge Univ. Press, 2013).
2. Post, E. et al. The polar regions in a 2 °C warmer world. *Sci. Adv.* **5**, eaaw9883 (2019).
3. Post, E. et al. Ecological dynamics across the Arctic associated with recent climate change. *Science* **325**, 1355–1358 (2009).
4. Schuur, E. A. G. et al. Climate change and the permafrost carbon feedback. *Nature* **520**, 171–179 (2015).
5. Schuur, E. A. G. et al. The effect of permafrost thaw on old carbon release and net carbon exchange from tundra. *Nature* **459**, 556–559 (2009).
6. McCalley, C. K. et al. Methane dynamics regulated by microbial community response to permafrost thaw. *Nature* **514**, 478–481 (2014).
7. Hicks Pries, C. E., Schuur, E. A. G., Natali, S. M. & Crummer, K. G. Old soil carbon losses increase with ecosystem respiration in experimentally thawed tundra. *Nat. Clim. Change* **6**, 214–218 (2016).
8. Schuur, E. A. G. et al. Vulnerability of permafrost carbon to climate change: implications for the global carbon cycle. *Bioscience* **58**, 701–714 (2008).
9. Jansson, J. K. & Taş, N. The microbial ecology of permafrost. *Nat. Rev. Microbiol.* **12**, 414–425 (2014).
10. Guillemette, F., Bianchi, T. S. & Spencer, R. G. M. Old before your time: ancient carbon incorporation in contemporary aquatic foodwebs. *Limnol. Oceanogr.* **62**, 1682–1700 (2017).
11. O'Donnell, J. A. et al. Permafrost hydrology drives the assimilation of old carbon by stream food webs in the Arctic. *Ecosystems* **23**, 435–453 (2020).
12. Berner, L. T. & Goetz, S. J. Satellite observations document trends consistent with a boreal forest biome shift. *Glob. Change Biol.* **28**, 3275–3292 (2022).
13. Berner, L. T. et al. Summer warming explains widespread but not uniform greening in the Arctic tundra biome. *Nat. Commun.* **11**, 4621 (2020).
14. Wirta, H. K. et al. Exposing the structure of an Arctic food web. *Ecol. Evol.* **5**, 3842–3856 (2015).
15. Steffan, S. A. & Dharampal, P. S. Undead food-webs: integrating microbes into the food-chain. *Food Webs* **18**, e00111 (2019).
16. Wolkovich, E. M. et al. Linking the green and brown worlds: the prevalence and effect of multichannel feeding in food webs. *Ecology* **95**, 3376–3386 (2014).
17. Manlick, P. J., Cook, J. A. & Newsome, S. D. The coupling of green and brown food webs regulates trophic position in a montane mammal guild. *Ecology* **104**, e3949 (2023).
18. Koltz, A. M., Asmus, A., Gough, L., Pressler, Y. & Moore, J. C. The detritus-based microbial–invertebrate food web contributes disproportionately to carbon and nitrogen cycling in the Arctic. *Polar Biol.* **41**, 1531–1545 (2018).
19. Summerhayes, V. S. & Elton, C. S. Contributions to the ecology of Spitsbergen and Bear Island. *J. Ecol.* **11**, 214–284 (1923).
20. Hodkinson, I. D. & Coulson, S. J. Are high Arctic terrestrial food chains really that simple? The Bear Island food web revisited. *Oikos* **106**, 427–431 (2004).
21. Zou, K., Thébault, E., Lacroix, G. & Barot, S. Interactions between the green and brown food web determine ecosystem functioning. *Funct. Ecol.* **30**, 1454–1465 (2016).
22. Schmitz, O. J. et al. Animating the carbon cycle. *Ecosystems* **17**, 344–359 (2014).
23. Schmitz, O. J. & Leroux, S. J. Food webs and ecosystems: linking species interactions to the carbon cycle. *Annu. Rev. Ecol. Evol. Syst.* **51**, 271–295 (2020).
24. Koltz, A. M., Gough, L. & McLaren, J. R. Herbivores in Arctic ecosystems: effects of climate change and implications for carbon and nutrient cycling. *Ann. N. Y. Acad. Sci.* **1516**, 28–47 (2022).
25. Leroux, S. J., Wiersma, Y. F. & Vander Wal, E. Herbivore impacts on carbon cycling in boreal forests. *Trends Ecol. Evol.* **35**, 1001–1010 (2020).
26. Olofsson, J., Tømmervik, H. & Callaghan, T. V. Vole and lemming activity observed from space. *Nat. Clim. Change* **2**, 880–883 (2012).
27. Pastor, J., Naiman, R. J., Dewey, B. & McInnes, P. Moose, microbes, and the boreal forest. *Bioscience* **38**, 770–777 (1988).
28. Wu, X., Duffy, J. E., Reich, P. B. & Sun, S. A brown-world cascade in the dung decomposer food web of an alpine meadow: effects of predator interactions and warming. *Ecol. Monogr.* **81**, 313–328 (2011).

29. Schmitz, O. J., Buchkowski, R. W., Smith, J. R., Telthorst, M. & Rosenblatt, A. E. Predator community composition is linked to soil carbon retention across a human land use gradient. *Ecology* **98**, 1256–1265 (2017).
30. Manlick, P. J. & Newsome, S. D. Stable isotope fingerprinting traces essential amino acid assimilation and multichannel feeding in a vertebrate consumer. *Methods Ecol. Evol.* **13**, 1819–1830 (2022).
31. Larsen, T., Taylor, D. L., Leigh, M. B. & O'Brien, D. M. Stable isotope fingerprinting: a novel method for identifying plant, fungal, or bacterial origins of amino acids. *Ecology* **90**, 3526–3535 (2009).
32. Larsen, T. et al. Tracing carbon sources through aquatic and terrestrial food webs using amino acid stable isotope fingerprinting. *PLoS ONE* **8**, e73441 (2013).
33. Sterner, R. W. & Elser, J. J. *Ecological Stoichiometry: The Biology of Elements from Molecules to the Biosphere* (Princeton Univ. Press, 2002).
34. Wendler, G. & Shulski, M. A century of climate change for Fairbanks, Alaska. *Arctic* **62**, 295–300 (2009).
35. Grodzinksi, W. Energy flow through populations of small mammals in Hie Alaskan Taiga Forest. *Acta Theriol.* **XVI**, 231–275 (1971).
36. Rexstad, E. & Kielland, K. In *Alaska's Changing Boreal Forest* (eds Chapin, F. S. III et al.) 121–132 (Oxford Univ. Press, 2006); https://doi.org/10.1093/oso/9780195154313.003.0013
37. Koltz, A. M., Classen, A. T. & Wright, J. P. Warming reverses top-down effects of predators on belowground ecosystem function in Arctic tundra. *Proc. Natl Acad. Sci. USA* **115**, E7541–E7549 (2018).
38. Koltz, A. M. & Wright, J. P. Impacts of female body size on cannibalism and juvenile abundance in a dominant Arctic spider. *J. Anim. Ecol.* **89**, 1788–1798 (2020).
39. Boonstra, R. & Krebs, C. J. Population dynamics of red-backed voles (*Myodes*) in North America. *Oecologia* **168**, 601–620 (2012).
40. Sistla, S. A. et al. Long-term warming restructures Arctic tundra without changing net soil carbon storage. *Nature* **497**, 615–617 (2013).
41. Moore, J. C. & Hunt, H. W. Resource compartmentation and the stability of real ecosystems. *Nature* **333**, 261–263 (1988).
42. Potapov, A. M. et al. Feeding habits and multifunctional classification of soil-associated consumers from protists to vertebrates. *Biol. Rev.* **97**, 1057–1117 (2022).
43. Hättenschwiler, S., Tiunov, A. V. & Scheu, S. Biodiversity and litter decomposition in terrestrial ecosystems. *Annu. Rev. Ecol. Evol. Syst.* **36**, 191–218 (2005).
44. Waldrop, M. P. et al. Molecular investigations into a globally important carbon pool: permafrost-protected carbon in Alaskan soils. *Glob. Change Biol.* **16**, 2543–2554 (2010).
45. Talbot, J. M., Allison, S. D. & Treseder, K. K. Decomposers in disguise: mycorrhizal fungi as regulators of soil C dynamics in ecosystems under global change. *Funct. Ecol.* **22**, 955–963 (2008).
46. Pokarzhevskii, A. D., Van Straalen, N. M., Zaboev, D. P. & Zaitsev, A. S. Microbial links and element flows in nested detrital food-webs. *Pedobiologia* **47**, 213–224 (2003).
47. Mizukami, N. et al. New projections of 21st century climate and hydrology for Alaska and Hawai'i. *Clim. Serv.* **27**, 100312 (2022).
48. Krebs, C. J., Carrier, P., Boutin, S., Boonstra, R. & Hofer, E. Mushroom crops in relation to weather in the southwestern Yukon. *Botany* **86**, 1497–1502 (2008).
49. Thormann, M. N., Bayley, S. I. & Currah, R. S. Microcosm tests of the effects of temperature and microbial species number on the decomposition of *Carex aquatilis* and *Sphagnum fuscum* litter from southern boreal peatlands. *Can. J. Microbiol.* **50**, 793–802 (2004).
50. Allison, S. D. & Treseder, K. K. Climate change feedbacks to microbial decomposition in boreal soils. *Fungal Ecol.* **4**, 362–374 (2011).
51. Thakur, M. P. Climate warming and trophic mismatches in terrestrial ecosystems: the green–brown imbalance hypothesis. *Biol. Lett.* **16**, 20190770 (2020).
52. Bartley, T. J. et al. Food web rewiring in a changing world. *Nat. Ecol. Evol.* **3**, 345–354 (2019).
53. Hobbie, E. A. et al. Stable Isotopes and Radiocarbon Assess Variable Importance of Plants and Fungi in Diets of Arctic Ground Squirrels. *Arctic, Antarct. Alp. Res.* **49**, 487–500 (2017).
54. Estop-Aragonés, C. et al. Assessing the potential for mobilization of old soil carbon after permafrost thaw: a synthesis of ^{14}C measurements from the northern permafrost region. *Glob. Biogeochem. Cycles* **34**, e2020GB006672 (2020).
55. Myers-Smith, I. H. et al. Complexity revealed in the greening of the Arctic. *Nat. Clim. Change* **10**, 106–117 (2020).

Methods

Sampling

We sampled bone collagen from small-mammal museum specimens of known provenance collected at boreal forest sites near the Bonanza Creek Long-Term Ecological Research (LTER) site in Fairbanks, Alaska (Supplementary Fig. 1 and Supplementary Appendix 1)[56], including tundra voles (*Microtus oeconomus*; $N_{1990} = 8, N_{2021} = 4$), red-backed voles (*Myodes rutilus*; $N_{1990} = 7, N_{2021} = 13$) and masked shrews (*Sorex cinereus*, $N_{1990} = 10, N_{2021} = 13$) collected in 1990 and 2021 by the University of New Mexico Museum of Southwestern Biology and the University of Alaska Museum of the North. All specimens were collected, handled and stored under standardized protocols[57,58], and sampling adhered to ethical guidelines outlined by the American Society of Mammalogists[59]. Wolf spiders were collected from experimental mesocosms in July 2013 after one summer of experimental warming designed to test effects of climate change and spider density on below-ground food webs near the Arctic LTER site at Toolik Lake, Alaska. Mesocosms were 1.5 m in diameter and enclosed with aluminium flashing that was buried 20 cm below ground and stood 20 cm above the soil surface. Half of the plots were experimentally warmed by covering the mesocosms with heavy-gauge plastic sheeting with regularly spaced openings; see ref. 38 for details. Daytime summer temperatures between ambient and warmed plots differed by approximately 2 °C (ref. 38). Wolf spiders for this study were collected from ambient-temperature ($N = 12$) and passively warmed ($N = 20$) mesocosms that had either control or high wolf spider densities. Lastly, we sampled plants ($N = 21$), fungi ($N = 1$) and soil from Fairbanks, Toolik Lake and Utqiagvik, Alaska, in summer 2021 to characterize green and brown energy sources (Supplementary Appendix 1)[56], and we cultured a subset of bacteria ($N = 2$) and fungi ($N = 2$) following ref. 17.

Stable isotope analysis

We analysed bone collagen from small mammals and whole-body samples from spiders. Bone collagen is a metabolically active but slowly integrating tissue that represents lifetime assimilated resources by small mammals[60], while whole-body tissues from spiders represent a combination of metabolically active tissues with high turnover rates (for example, internal organs and haemolymph) and metabolically inert tissues that represent a brief window of assimilation (for example, chitin). However, chitin does not contain amino acids; therefore, our analyses largely capture the isotopic composition of metabolically active tissues and represent a period of several weeks before capture. We measured amino acid $\delta^{13}C$ values for 55 small mammals, 32 spiders and 26 sources (Supplementary Appendix 1)[56]. Consumer and source tissues were hydrolysed and derivatized to N-trifluoroacetic acid isopropyl esters for analysis via gas chromatography combustion isotope ratio mass spectrometry (GC-C-IRMS) following established protocols[17,61]. All samples were analysed in duplicate and bracketed by internal reference material used to correct measured $\delta^{13}C$ values following ref. 62 (Supplementary Table 2). We measured $\delta^{13}C$ values of 14 amino acids, and we report isotope data in δ-notation as parts per mil (‰) relative to the international standard Vienna PeeDee Belemnite. We conducted 22 GC-C-IRMS runs with 95 reference injections ($\bar{x} = 4.3$ per run) and mean within-run standard deviation of reference material was ≤0.47‰ ($\bar{x} = 0.25$‰) for the six EAAs used in $\delta^{13}C$ fingerprinting (Supplementary Table 2). All analyses were conducted at the University of New Mexico Center for Stable Isotopes. See Supplementary Information 'Protocols' for detailed analytical methods.

EAA $\delta^{13}C$ fingerprinting

We used $\delta^{13}C$ fingerprinting[30,31] to quantify C assimilation by consumers, focusing on six EAAs: isoleucine, leucine, lysine, phenylalanine, threonine and valine. We combined measured values with published EAA $\delta^{13}C$ data[31,32] for plants ($n = 5$), fungi ($n = 13$) and bacteria ($n = 10$) collected in boreal forest near Fairbanks, Alaska (Supplementary Appendix 1)[56]. We characterized $\delta^{13}C$ fingerprints using linear discriminant analysis (LDA)[30,31] and trained the LDA using EAA $\delta^{13}C$ data for plant, fungal and bacterial sources. We also included filamentous green algae as a potential source of aquatic C (refs. 63), but we found no evidence of algal C assimilation by consumers and therefore removed this potential source to create a more parsimonious mixing space. Models for boreal mammals included only sources collected near Fairbanks, Alaska, while models for spiders included sources from Fairbanks, Arctic LTER (Toolik Lake, Alaska) and Barrow, Alaska, due to limited data on sources from the Arctic. All EAA $\delta^{13}C$ values for sources and consumers were Suess-corrected to modern values following Dombrosky[64]. We used leave-one-out cross-validation to show that source classification accuracy was high for both the boreal model (94.6%) and the Arctic model (94.2%; Supplementary Table 2) and then predicted group assignment for consumers. All analyses were completed in the r package mass (v.7.3-54)[65].

Food webs and energy channelling

To quantify shifts in energy channel assignment, we used PERMANOVAs with 10,000 permutations to test for differences in mean predicted first and second LDA coordinates between periods (mammals) and experimental treatments (spiders) using the r package vegan (v.2.5-7)[66]. We then used Bayesian mixing models in the r package simmr (v.0.4.5)[67] to quantify the proportional assimilation of C from energy channels by consumers[30] (see Supplementary Information 'Protocols'). We parameterized source and consumer mixtures using LDA coordinates and grouped consumers by period (mammals) or treatment (spiders), with separate models run for mammals and spiders. To test for significant differences between groups, we extracted the marginal posterior distributions and calculated the two-sided probability that the difference between marginal posterior distributions was less than zero[68,69] (see Supplementary Information 'Protocols'). This is analogous to a *t* test for posterior distributions, and we used Benjamini–Hochberg false discovery rate correction to assess significance at $\alpha = 0.05$, 0.01 and 0.001. We found no effect of spider density (all $P > 0.50$) on C assimilation and report only warming effects herein.

Radiocarbon dating

We radiocarbon (^{14}C) dated bone collagen from three to four individual mammals per species per period ($N = 18$) via accelerator mass spectrometry (AMS) at the Pennsylvania State University's Radiocarbon Lab (see Supplementary Information 'Protocols'). Individuals were selected by identifying animals with the most assimilated brown carbon in each period, as identified by mixing models. Samples were run on a National Electronics Corporation compact AMS with a 0.5 MV accelerator. Analytical error is in the 2–3‰ range for near-modern samples under currents of up to 200 µA of ^{12}C- and routinely generating 120–150 µA of ^{12}C- from ~0.7 mgC samples. Radiocarbon ages are corrected for mass-dependent fractionation with $\delta^{13}C$ values measured on the AMS, normalized to an oxalic acid standard (OXII, SRM-4990C), and reported as $\Delta^{14}C$ (‰), or the deviation of ^{14}C:^{12}C in the sample relative to the standard. All data were calibrated to the NHZ1 post-bomb calibration curve using CALIBomb software[70] and results are reported as $\Delta^{14}C$ (‰). Differences between bone collagen and monthly atmospheric $\Delta^{14}C$ values from NHZ1 for the same time periods (reported by Hua et al.)[71] were determined via two-sided *t* tests with animals from 2021 compared to 2019, the most recent atmospheric $\Delta^{14}C$ values available.

Carbon pools and fluxes

We estimated changes in carbon storage due to food-web shifts using the equation $(P_{bac} + P_{fun}) \times C \times D \times M$, where P_{bac} and P_{fun} are the estimated mean proportions of assimilated bacteria and fungi, respectively, C is the weight percent carbon in animal tissues, D is consumer density (animals m^{-2}) and M is the average mass (g) of the consumer. For

M. rutilus, we populated the equation using mixing model posteriors for P_{bac} and P_{fun} and we calculated weight percent carbon from bulk tissue measurements of bone collagen via EA-IRMS (Supplementary Appendix 1)[56]. We estimated density using combined means of *M. rutilus* from population studies near Fairbanks, Alaska[39], and we calculated average mass using >1,000 individual *M. rutilus* measurements from 2017 to 2022 collected by the National Ecological Observatory Network on the nearby Bonanza Creek LTER site. For spiders, we used the same approach to estimate P_{bac}, P_{fun} and C, and we used combined mass and density estimates from ref. 37 to parameterize the equation. Because the majority of vertebrate biomass is bound in proteins[33], and EAA $\delta^{13}C$ fingerprints accurately estimate crude protein assimilation[30], our approach provides a reasonable proxy for assimilated C in mammals. We assumed that the assimilation of C in spiders, including chitinous exoskeletons, was comparable to protein assimilation by mammals. For both estimates, we propagated error using a Monte Carlo simulation (100,000 iterations) in the r package propagate (v.1.0-6)[72].

Reporting summary

Further information on research design is available in the Nature Portfolio Reporting Summary linked to this article.

Data availability

All data[56] used in this study are publicly archived at https://figshare.com/s/4eb07f4001aadc9a9a37, https://doi.org/10.6084/m9.figshare.22975145.

Code availability

All code[56] used in this study[72] is publicly archived at https://figshare.com/s/4eb07f4001aadc9a9a37, https://doi.org/10.6084/m9.figshare.22975145.

References

56. Manlick, P. J., Perryman, N. L., Koltz, A. M., Cook, J. A. & Newsome, S. D. Data from: 'Climate warming restructures food webs and carbon flow in high-latitude ecosystems'. *Figshare* https://doi.org/10.6084/m9.figshare.22975145 (2023).
57. Yates, T. L., Jones, C. & Cook, J. A. In *Measuring and Monitoring Biological Diversity: Standard Methods for Mammals* (eds Wilson, E. et al.) 265–273 (Smithsonian Institution Press, 1996).
58. Galbreath, K. E. et al. Building an integrated infrastructure for exploring biodiversity: field collections and archives of mammals and parasites. *J. Mammal.* **100**, 382–393 (2019).
59. Sikes, R. S. 2016 Guidelines of the American Society of Mammalogists for the use of wild mammals in research and education. *J. Mammal.* **97**, 663–688 (2016).
60. Dalerum, F. & Angerbjörn, A. Resolving temporal variation in vertebrate diets using naturally occurring stable isotopes. *Oecologia* **144**, 647–658 (2005).
61. Silfer, J. A., Engel, M. H., Macko, S. A. & Jumeau, E. J. Stable carbon isotope analysis of amino acid enantiomers by conventional isotope ratio mass spectrometry and combined gas chromatography/isotope ratio mass spectrometry. *Anal. Chem.* **63**, 370–374 (1991).
62. O'Brien, D. M., Fogel, M. L. & Boggs, C. L. Renewable and nonrenewable resources: amino acid turnover and allocation to reproduction in Lepidoptera. *Proc. Natl Acad. Sci. USA* **99**, 4413–4418 (2002).
63. Besser, A. C., Elliott Smith, E. A. & Newsome, S. D. Assessing the potential of amino acid $\delta^{13}C$ and $\delta^{15}N$ analysis in terrestrial and freshwater ecosystems. *J. Ecol.* **110**, 935–950 (2022).
64. Dombrosky, J. A ~1000-year ^{13}C Suess correction model for the study of past ecosystems. *Holocene* **30**, 474–478 (2020).
65. Ripley, B. et al. Package 'mass' v.7.3-60 (2013).
66. Oksanen, J. et al. Package 'vegan'. Community ecology package v.2.9 (2013).
67. Parnell, A. C. & Inger, R. Simmr: a stable isotope mixing model. R package v.0.3 (2016).
68. Hopkins, J. B., Koch, P. L., Ferguson, J. M. & Kalinowski, S. T. The changing anthropogenic diets of American black bears over the past century in Yosemite National Park. *Front. Ecol. Environ.* **12**, 107–114 (2014).
69. Manlick, P. J., Petersen, S. M., Moriarty, K. M. & Pauli, J. N. Stable isotopes reveal limited Eltonian niche conservatism across carnivore populations. *Funct. Ecol.* **33**, 335–345 (2019).
70. Reimer, R. W. & Reimer, P. J. CALIBomb (2022).
71. Hua, Q. et al. Atmospheric radiocarbon for the period 1950–2019. *Radiocarbon* **64**, 723–745 (2022).
72. Spiess, A. propagate: Propagation of Uncertainty (2018).

Acknowledgements

We thank A. Martinez for laboratory assistance and L. Berner for reviewing an early version of this manuscript. P.J.M. was supported by NSF (DBI- 2010712) and the USFS Pacific Northwest Research Station, with in-kind support from UNM-CSI and UNM-MSB. A.M.K. was supported by NSF (DEB-1210704) and the National Geographic Committee for Research and Exploration.

Author contributions

P.J.M., N.L.P. and S.D.N. conceived of the study, and all authors collected data. P.J.M. and N.L.P. conducted laboratory and statistical analyses, and P.J.M. wrote the first draft of the manuscript. All authors contributed substantially to revisions.

Competing interests

The authors declare no competing interests.

Additional information

Supplementary information The online version contains supplementary material available at https://doi.org/10.1038/s41558-023-01893-0.

Correspondence and requests for materials should be addressed to Philip J. Manlick.

Peer review information *Nature Climate Change* thanks Emily Arsenault, Matthias Pilecky and Ryan Stephens for their contribution to the peer review of this work.

nature portfolio

Corresponding author(s): Manlick, Philip J.

Last updated by author(s): Oct 11, 2023

Reporting Summary

Nature Portfolio wishes to improve the reproducibility of the work that we publish. This form provides structure for consistency and transparency in reporting. For further information on Nature Portfolio policies, see our Editorial Policies and the Editorial Policy Checklist.

Statistics

For all statistical analyses, confirm that the following items are present in the figure legend, table legend, main text, or Methods section.

n/a	Confirmed	
☐	☒	The exact sample size (*n*) for each experimental group/condition, given as a discrete number and unit of measurement
☐	☒	A statement on whether measurements were taken from distinct samples or whether the same sample was measured repeatedly
☐	☒	The statistical test(s) used AND whether they are one- or two-sided *Only common tests should be described solely by name; describe more complex techniques in the Methods section.*
☐	☒	A description of all covariates tested
☐	☒	A description of any assumptions or corrections, such as tests of normality and adjustment for multiple comparisons
☐	☒	A full description of the statistical parameters including central tendency (e.g. means) or other basic estimates (e.g. regression coefficient) AND variation (e.g. standard deviation) or associated estimates of uncertainty (e.g. confidence intervals)
☐	☒	For null hypothesis testing, the test statistic (e.g. *F*, *t*, *r*) with confidence intervals, effect sizes, degrees of freedom and *P* value noted *Give P values as exact values whenever suitable.*
☐	☒	For Bayesian analysis, information on the choice of priors and Markov chain Monte Carlo settings
☒	☐	For hierarchical and complex designs, identification of the appropriate level for tests and full reporting of outcomes
☒	☐	Estimates of effect sizes (e.g. Cohen's *d*, Pearson's *r*), indicating how they were calculated

Our web collection on statistics for biologists contains articles on many of the points above.

Software and code

Policy information about availability of computer code

Data collection	Isotopic data were acquired using Isodat 3.0 Software (Thermo Fisher Scientific).
Data analysis	All analyses were conducted in the R statistical platform as described in Methods.

For manuscripts utilizing custom algorithms or software that are central to the research but not yet described in published literature, software must be made available to editors and reviewers. We strongly encourage code deposition in a community repository (e.g. GitHub). See the Nature Portfolio guidelines for submitting code & software for further information.

Data

Policy information about availability of data

All manuscripts must include a data availability statement. This statement should provide the following information, where applicable:

- Accession codes, unique identifiers, or web links for publicly available datasets
- A description of any restrictions on data availability
- For clinical datasets or third party data, please ensure that the statement adheres to our policy

All data used in this study is publicly archived at https://figshare.com/s/4eb07f4001aadc9a9a37, doi:10.6084/m9.figshare.22975145.

Research involving human participants, their data, or biological material

Policy information about studies with human participants or human data. See also policy information about sex, gender (identity/presentation), and sexual orientation and race, ethnicity and racism.

Reporting on sex and gender	N/A
Reporting on race, ethnicity, or other socially relevant groupings	N/A
Population characteristics	N/A
Recruitment	N/A
Ethics oversight	N/A

Note that full information on the approval of the study protocol must also be provided in the manuscript.

Field-specific reporting

Please select the one below that is the best fit for your research. If you are not sure, read the appropriate sections before making your selection.

☐ Life sciences ☐ Behavioural & social sciences ☒ Ecological, evolutionary & environmental sciences

For a reference copy of the document with all sections, see nature.com/documents/nr-reporting-summary-flat.pdf

Ecological, evolutionary & environmental sciences study design

All studies must disclose on these points even when the disclosure is negative.

Study description	We measured δ13C values in individual amino acids from plants, bacteria, fungi and animals (small mammals, spiders) to quantify carbon flow and assess the impact of warming on Boreal forest and Arctic tundra food webs.
Research sample	We measured amino acid δ13C values for 55 small mammal museum specimens, 32 spiders from experimental mesocosms, and 26 sources (plants, bacteria, and fungi) opportunistically collected near Fairbanks, AK and Toolik Lake, AK. Previously published data from sources (N=26) were gathered from Larsen et al. 2009. Radiocarbon (14C) data was derived from 18 small mammals to age the source of carbon.
Sampling strategy	Specimens of each species were identified in the Arctos Database for each mammal species and sampled as available following standardized destructive sampling protocols. Spiders were sampled based on biomass available for isotopic analysis (>0.5mg dry). Specimens were identified for 14C analysis based on the proportion of microbial carbon assimilated, as identified by stable isotope mixing models.
Data collection	All specimens were collected, handled, and stored under standardized museum protocols, with associated data (e.g., date, locality, standard measurements). Skeletons were sampled based on biomass and bone collagen was isolated following Methods. Spiders were collected and stored in ethanol, while sources were collected and lyopholized for long-term storage at room temperature.
Timing and spatial scale	Small mammal specimens were collected in fall of 1990 and summer 2021 along standardized traplines near Fairbanks, Alaska (Fig S1). Spiders were sampled from 1.5 m diameter experimental mesocosms (warmed, ambient) in July 2013.
Data exclusions	Previously published data on sources (e.g., plants, fungi) were excluded if they were cultivars, only field collected specimens were used in analyses.
Reproducibility	Experimental mesocosms were replicated across 3 summers (Koltz et al. 2018, Koltz et al. 2020, see Methods). All isotopic analyses were run in duplicate, and all statistical approaches are available in archived R code.
Randomization	Samples were allocated into groups based on taxonomy (species [mammals], sources [plant, bacteria, fungi]), year collected (1990, 2021), and experimental treatment (warmed, ambient).
Blinding	Blinding was not applied as it did not involve participants.

Did the study involve field work? ☒ Yes ☐ No

Field work, collection and transport

Field conditions	The Fairbanks study area is in interior Alaska and characterized by cold winters and warm, relatively dry summers. There are drastic fluctuation in day length across seasons (> 21 hours on June 21 and < 3 hours on December 21). Mean annual temperatures in the area average between -2 and -5 °C. July temperatures average 16.3 °C, whereas in January the average is -23.5 °C. Annual precipitation is 250 to 500 mm, with ~35% falling between October and April as snow. Snow covers the ground from mid-October until mid- to late April, and maximum accumulation averages 75 to100 cm. Soil temperatures are consistently low and soils are uniformly immature and range from cold poorly drained soils with shallow permafrost to warm well-drained soils in the uplands that support mature white spruce communities. Vegetation is taiga forest and consists of a mosaic of forest, grassland, shrubs, bogs, and alpine tundra. The Toolik Lake Study area is located in the northern foothills of Alaska's Brooks Range and the climate is characterized by long, cold winters; short, cool summers; and extreme seasonal variation. Toolik Lake has an average mean temperature of -9°C (16°F) and it receives a mean annual precipitation of 316 mm (12.4 in). Winter temperatures can reach -40°C or lower, and summer is the only time of year where average temperatures exceed 0°C (32°F). Soils in the Arctic tundra include discontinuous permafrost and vegetation is mainly shrubs and herbaceous flowering plants, including willows (Salix spp.), blueberry (Vaccinium uliginosum), and dwarf birch (Betula nana).
Location	Small mammals were collected near Fairbanks, AK and spiders in Toolik, Lake AK. Exact coordinates included in archived data at doi:10.6084/m9.figshare.22975145
Access & import/export	All samples and specimens were acquired from previously published research or museum archives and accession was provided by A. Koltz, University of Alaska Museum of the North, and UNM Museum of Southwestern Biology.
Disturbance	The study did not cause any obvious disturbance to selected sites

Reporting for specific materials, systems and methods

We require information from authors about some types of materials, experimental systems and methods used in many studies. Here, indicate whether each material, system or method listed is relevant to your study. If you are not sure if a list item applies to your research, read the appropriate section before selecting a response.

Materials & experimental systems

n/a	Involved in the study
☒	☐ Antibodies
☒	☐ Eukaryotic cell lines
☒	☐ Palaeontology and archaeology
☐	☒ Animals and other organisms
☒	☐ Clinical data
☒	☐ Dual use research of concern
☒	☐ Plants

Methods

n/a	Involved in the study
☒	☐ ChIP-seq
☒	☐ Flow cytometry
☒	☐ MRI-based neuroimaging

Animals and other research organisms

Policy information about studies involving animals; ARRIVE guidelines recommended for reporting animal research, and Sex and Gender in Research

Laboratory animals	No laboratory animals were used.
Wild animals	All animals were acquired from museum archives or previously published experiments and associated metadata is included in archived data at doi:10.6084/m9.figshare.22975145.
Reporting on sex	Sex of organisms/specimens was not always known, thereby precluding sex-based comparisons. Data on age and sex are included in archived data at doi:10.6084/m9.figshare.22975145
Field-collected samples	Samples were collected in the field as described in Methods and all associated metadata is archived at doi:10.6084/m9.figshare.22975145
Ethics oversight	No ethical approval was required for this study because all vertebrate specimens were acquired from archived museum specimens. Sampling of organisms by UAM and MSB nevertheless adhered to the ethical guidelines outlined by the American Society of Mammalogists.

Note that full information on the approval of the study protocol must also be provided in the manuscript.

Plants

Seed stocks	No seed stocks were used.
Novel plant genotypes	No plant genotypes were assessed.
Authentication	N/A